Thermal conductivity of strongly coupled Yukawa liquids

Z. Donkó and P. Hartmann
Research Institute for Solid State Physics and Optics of the Hungarian Academy of Sciences, P.O. Box 49, H-1525 Budapest, Hungary
(Received 15 August 2003; published 28 January 2004)

The thermal conductivity of strongly coupled Yukawa liquids, being relevant to dusty plasmas, is calculated from nonequilibrium molecular dynamics simulations. The calculations cover a wide range of plasma coupling (Γ) and screening (κ) parameters and yield data which are generally in good agreement with the results of recent independent calculations. An improved analytical formula, relating the thermal conductivity to the reduced temperature and to the screening length, is proposed.

DOI: 10.1103/PhysRevE.69.016405 PACS number(s): 52.27.Gr, 52.25.Fi, 52.27.Lw

I. INTRODUCTION

The first set of data for the transport parameters (self-diffusion coefficient, shear and bulk viscosities, and thermal conductivity) of strongly coupled one-component plasmas (OCP) have been derived in the 1970s from theoretical calculations [1–3] and from computer simulations [4]. The self-diffusion coefficient D was found to be a monotonically decreasing function of the coupling strength of the plasma, $\Gamma=(Q^2/4\pi\varepsilon_0)(1/ak_BT)$, where Q is the charge of the particles, T is the temperature, $a=(4n\pi/3)^{-1/3}$ is the Wigner-Seitz (WS) radius, and n is the density of particles. In contrast with the behavior of D, it was also shown that the shear viscosity η exhibits a minimum at intermediate values of the coupling coefficient, $\Gamma\approx 10$, and that the bulk viscosity is orders of magnitude lower compared to the shear viscosity. The first computer simulation results for the thermal conductivity λ have been obtained only for a few Γ values [4], but already suggested that λ has a minimum at around the same value of Γ, as the shear viscosity.

More detailed data for the shear viscosity and the thermal conductivity of the classical OCP have been obtained from recent nonequilibrium (transient) molecular dynamics (MD) simulations [5,6]. These simulations were based on the measurement of the relaxation time of the ensemble of particles after introducing a specific perturbation to the system. In the case of thermal conductivity ''measurements'' a sinusoidal temperature profile was imposed on the system and the relaxation of this profile was monitored. For the calculations of the shear viscosity the decay of the perturbation of the velocity field was measured [6]—these simulations have confirmed the results of the earlier calculations of η, both in terms of the Γ value where η has its minimum, and the value of $\eta_{\min}$. Simulations aiming the determination of the thermal conductivity [5,6] confirmed that λ has a minimum at $\Gamma\approx 10-15$.

In the last few years increased attention has been devoted to particle systems interacting through the screened Coulomb (Yukawa) potential, due to the relevance of this model system to dusty plasmas. Self-diffusion properties of Yukawa systems have been explored by Ohta and Hamaguchi [7] and Liu *et al.* [8]. The shear viscosity was studied by Sanbonmatsu and Murillo [9] and Saigo and Hamaguchi [10]. The results for η presented in Ref. [10] in the low-screening limit confirmed the nonequilibrium MD results of Donkó *et al.* [5,6]. Very recent comprehensive studies of Yukawa transport coefficients by Salin and Caillol [11,12] and by Faussurier and Murillo [13] indicate current interest in the subject.

The aim of this paper is to present calculations of the thermal conductivity of Yukawa systems, based on a different simulation method than those used previously. The calculations are carried out for a wide range of characteristic parameters of the system (wider range of Γ than in any previous work), and the results are compared with those derived in recent independent calculations [12,13].

Section II of the paper describes the simulation technique and Sec. III presents the results and their comparison with data published by other authors. The work is summarized in Sec. IV.

II. SIMULATION METHOD

The motion of the particles in the system is described by molecular dynamics simulation. N simulation particles are contained in a cubic computational box having periodic boundary conditions in all three space dimensions, and they interact through the Yukawa potential

$$\phi(r)=\frac{Q^2}{4\pi\varepsilon_0}\frac{\exp(-r/\lambda_D)}{r}, \tag{1}$$

where λ_D is the Debye (screening) length. The screening parameter $\kappa=a/\lambda_D$, together with the coupling parameter Γ, fully characterizes the equilibrium system. In the $\kappa\to 0$ limit the interaction reduces to the $1/r$ Coulomb type (OCP limit).

The calculation of the thermal conductivity is based on the nonequilibrium molecular dynamics (NEMD) approach introduced by Müller-Plathe [14]. The simulation box is divided into several slabs along one of the axes (x axis in our case) and two of the slabs are assigned to be the ''cold slab'' and a ''hot slab,'' as illustrated in Fig. 1. In each kth simulation time step the fastest particle in the cold slab and slowest particle in the hot slab are searched for and their momenta are exchanged. This artificial perturbation of the system creates a heat flux between the hot and the cold slabs and gives rise to a specific spatial temperature profile throughout the system [14].

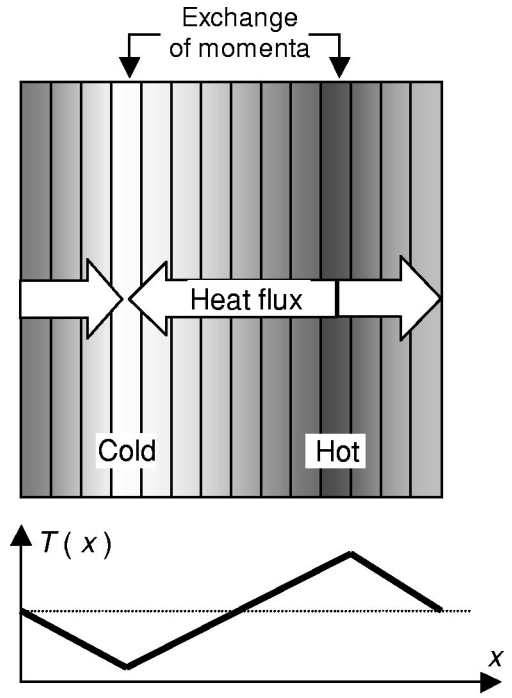

FIG. 1. Illustration of the nonequilibrium molecular dynamics simulation method originally proposed by Müller-Plathe [14]. Lighter and darker colors indicate colder and hotter parts of the simulation box. The exchange of particles' momenta between the cold and hot slabs results in a heat flux and a temperature gradient, which is shown in the lower part of the figure.

At the initialization of the simulation the particles are loaded at randomly chosen positions into the cubic computational box. Their initial velocities are randomly directed with magnitudes sampled from a Maxwellian distribution corresponding to the specified value of Γ. In a number of initial time steps the velocities of the particles are slightly adjusted to eliminate the possible small drift of the system, i.e., to ensure that $\langle v_x\rangle=\langle v_y\rangle=\langle v_z\rangle=0$ ($\langle\cdot\rangle$ denotes averaging over the ensemble of particles). The perturbation giving rise to the spatial temperature profile (as explained above) is applied from the beginning of the simulation and the system is given sufficient time (10 000 and 5000 time steps, respectively, in the case of $N=1600$ and 6400 particles) to relax to the stationary (perturbed) state before the measurement (data collection) phase starts. During this initial phase of the simulation the momenta of the particles are regularly rescaled in order to keep the average temperature of the system at the desired value. The number of simulation time steps in the data collection phase is 5×10^5 for $N=1600$ and ranges between 5×10^4 and 1×10^5 for $N=6400$. For these conditions $\omega_p t$ (where $\omega_p=\sqrt{Q^2n/\varepsilon_0 m}$ is the plasma frequency) is in the order of several thousands. The above momentum-rescaling procedure is also applied during the data collection phase, however, only in every 5000th time step, to compensate for the long term accumulation of numerical errors. (It is noted that the system temperature during the data collection phase does not rise in an observable way even without this additional thermostation.)

During the data collection phase of the simulation the spatial and temporal average of the temperature gradient $\langle\Delta T/\Delta x\rangle$ between the cold and hot slabs is measured and the thermal conductivity is calculated as

$$\lambda=\frac{E}{2St\left\langle\frac{\Delta T}{\Delta x}\right\rangle}, \tag{2}$$

where E is the (cumulative) energy exchanged between the hot and cold slabs during the runtime of the simulation t and $S=L^2$ is the cross sectional area of the simulation box. This NEMD technique has already been successfully applied to calculations of thermal conductivity of Lennard-Jones and molecular fluids [14–16].

The thermal conductivity resulting from Eq. (2) can conveniently be expressed in reduced units. Most common are the normalizations by the plasma frequency ω_p or by the Einstein frequency ω_E [13], respectively

$$\lambda'=\frac{\lambda}{nk_B\omega_p a^2} \quad \lambda^*=\frac{\lambda}{nk_B\sqrt{3}\omega_E a^2}, \tag{3}$$

where ω_E is the oscillation frequency of a particle around its equilibrium position when all other particles are at their equilibrium lattice sites, see, e.g., Ref. [7]. The Einstein frequency decreases with increasing κ, from a value $\omega_E=\omega_p/\sqrt{3}$ at $\kappa=0$ [7]. Here we follow the notation used in Ref. [13], while in our earlier work [5,6] and in Ref. [12] $\lambda/nk_B\omega_p a^2$ was denoted by λ^*.

III. RESULTS

Our simulations are carried out with number of particles chosen to be $N=1600$ and $N=6400$. These two different settings make it possible to investigate system size effects. The simulation box is divided into 32 slabs.

The temperature gradient establishing in the system depends on the frequency of perturbations. This way—by exchanging the momenta of the two selected particles in the cold and hot slabs relatively rarely—arbitrarily small temperature gradients can be established, causing very small perturbation to the system. However, at very low $\Delta T/\Delta x$ noise may be dominant, thus a proper choice of the delay between momenta exchanges is a compromise between the degree of perturbation and signal to noise ratio of the quantities (E/t and $\Delta T/\Delta x$) to be measured. In Fig. 2 the $T(x)$ profiles are plotted for different values of k (number of time steps between momenta exchanges), $k=75$, 150, and 300. The $T(x)$ profiles are very nearly linear, with a slope $\Delta T/\Delta x$ depending on k. In the further simulations the frequency of the exchange of momenta between the selected particles in the cold and hot slabs is chosen to be between $k=50$ and 300 time steps, to result in a $\lesssim\pm10\%$ perturbation of the temperature profile.

The results of our calculations for the thermal conductivity normalized by the plasma frequency λ' are shown in Fig. 3 for $\kappa=0.1$, and in Fig. 4 for $\kappa=1$, 2, and 3. Figures 3 and

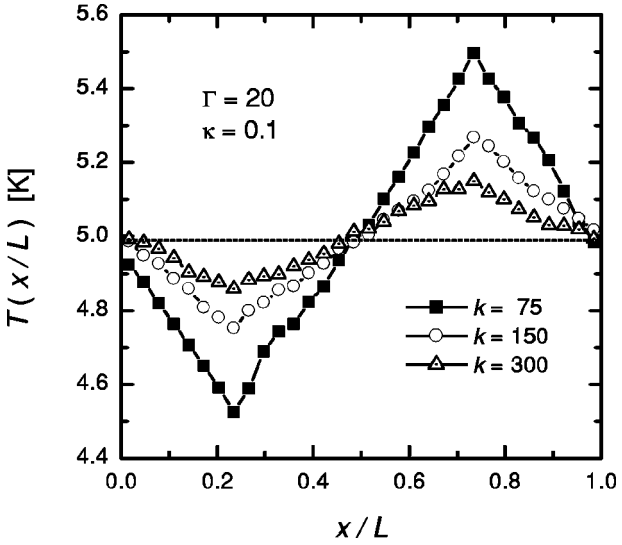

FIG. 2. Spatial temperature profiles obtained at $\Gamma=20$, $\kappa=0.1$, for different number of time steps (k) between artificial changes of particle momenta in the cold and hot slabs, situated at $x/L = 0.25$ and 0.75, respectively.

4 also include the data published by Salin and Caillol [12] and a universal functional form for the thermal conductivity proposed by Faussurier and Murillo [13]

$$\lambda^*=0.01176T^*+\frac{0.881}{T^*}+0.1655, \tag{4}$$

converted to λ' as $\lambda'=\lambda^*(\sqrt{3}\omega_E/\omega_p)$, where the normalized temperature $T^*=\Gamma_c/\Gamma$, with Γ_c being the coupling

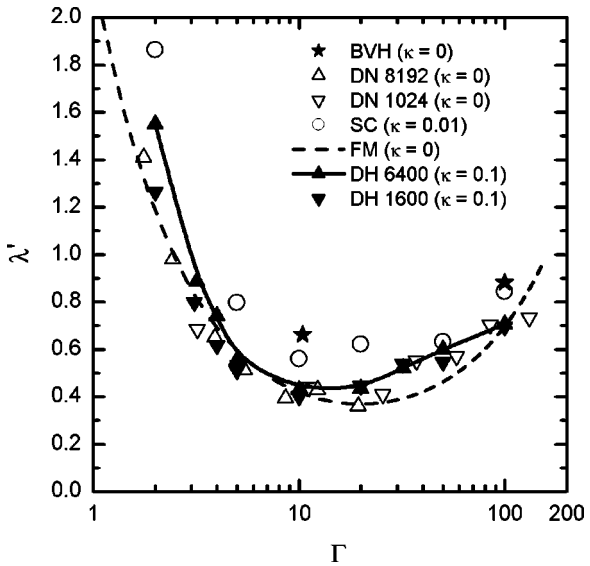

FIG. 3. Reduced thermal conductivity [normalized by the plasma frequency (3)] for $0\leqslant\kappa\leqslant0.1$—the precise values are given in the legend. Bernu, Viellefoss, and Hansen (BVH) [4], Donkó and Nyíri (DN) [6] (obtained with 8192 and 1024 particles), Salin and Caillol (SC) [12], Faussurier and Murillo (FM) [13], and Donkó and Harmann (DH): present results (with 6400 and 1600 particles). Note that $\lambda^*\simeq\lambda'$ at $\kappa\approx0$.

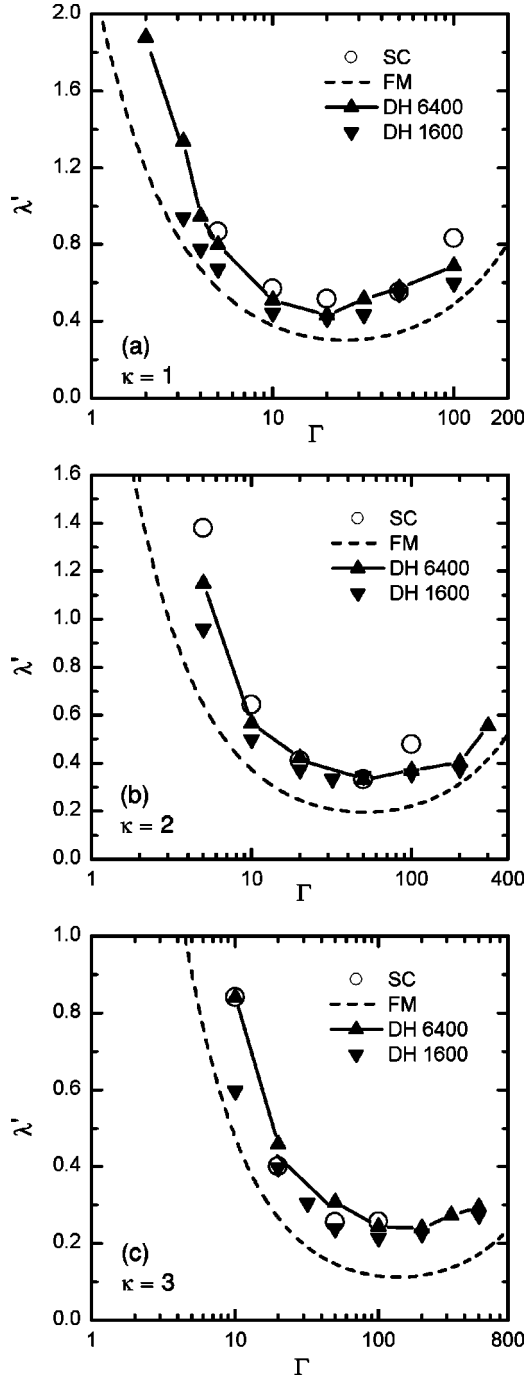

FIG. 4. Reduced thermal conductivity [normalized by the plasma frequency (3)] at (a) $\kappa=1$, (b) $\kappa=2$, and (c) $\kappa=3$. Salin and Caillol (SC) [12] and Faussurier and Murillo (FM) [13], and Donkó and Harmann (DH): present results (with 6400 and 1600 particles).

strength corresponding to melting (which, as a function of κ is given in Ref. [17]). This functional form was found to describe properly the scaling properties of the shear viscosity, as explored by Saigo and Hamaguchi [10]. Additionally, Fig. 3 also shows the data given in Refs. [5,6] for the Coulomb OCP, obtained with a different simulation technique.

In the limit of small κ (see Fig. 3) the result of the present simulations agree well with the Coulomb OCP data [5,6],

especially at the higher Γ values. These two sets of data also agree in terms of the position of the minimum of λ' (occurring at $\Gamma \cong 10$–15) as well as of the value $\lambda'_{\min} \cong 0.4$. At the lowest Γ values the present simulations give a slightly ($\approx 10\%$) higher λ', compared to Refs. [5,6]. Around the minimum position, at $\Gamma = 10$ the present value is well below the result of Bernu *et al.* [4]. At $\Gamma = 100$ the difference is still about 20%. The data of Salin and Caillol [12] lie between the present data and those of Ref. [4]; they are 20–30 % higher compared to the present results. At $\kappa \approx 0$ the fit (4) approximates well the present data, especially at intermediate values of Γ.

The results obtained at the higher κ values are shown in Fig. 4. The present data indicate that the position of the minimum of λ' shifts towards higher Γ as κ increases. The minimum value of λ' decreases with increasing κ, to $\lambda'_{\min} \cong 0.24$ at $\kappa = 3$. (It is noted that the thermal conductivity normalized by the Einstein frequency λ^* increases with increasing κ, to a value $\lambda^*_{\min} \cong 0.8$ at $\kappa = 3$.) The data are generally in a good agreement with the results of Salin and Caillol [11,12] given for $\Gamma \leqslant 100$ range. At high κ and $\Gamma > 100$ the thermal conductivity exhibits an increasing tendency with increasing Γ, similarly to the $\kappa \cong 0$ case. The analytical formula (4) reproduces well the shift of the position of $\lambda'_{\min}$ with increasing κ. The agreement between the calculated $\lambda'_{\min}$ values and those given by Eq. (4) is not very good, in the worst case, at $\kappa = 3$, the data differ by a factor of 2. The simulation results obtained with $N = 6400$ and 1600 particles agree within the limits of errors at high Γ values, but deviate at the lower values of Γ. This deviation shows up at increasingly higher values of Γ when κ increases (from $\Gamma \approx 3$ at $\kappa = 0.1$ to $\Gamma \approx 20$ at $\kappa = 3$).

We believe that the system size (N) dependence of the results at low coupling values originates from the long trajectory segments where particle motion is unperturbed by the other particles. In other words, the simulation scheme is expected to be valid as long as the characteristic size of the system is bigger than the length scale for interaction (significant exchange of momenta) between the particles. This latter can be quantitatively studied by calculating the velocity autocorrelation function of the system $A_{\mathbf{vv}}$ (already discussed in Ref. [7] for Yukawa systems) and its decay for different Γ and κ values. Figure 5 shows $A_{\mathbf{vv}}$ functions defined as

$$A_{\mathbf{vv}}(t) = \frac{\langle \mathbf{v}(t) \cdot \mathbf{v}(t_0 + t) \rangle}{\langle \mathbf{v}(t_0) \cdot \mathbf{v}(t_0) \rangle}, \tag{5}$$

where $\langle\rangle$ denotes averaging over particles and different initial times t_0. At high Γ values $A_{\mathbf{vv}}$ exhibits a fast decay as illustrated in Fig. 5(a) for the $\kappa = 0.1$ case. The decay time τ of $A_{\mathbf{vv}}$, defined as $A_{\mathbf{vv}}(t = \tau) = 1/\epsilon$ ($\epsilon = 2.718$) increases as Γ is decreased. The time needed for a particle to proceed a distance L (where L is the edge length of the simulation box) is $\Delta t = L/\overline{v}$, where $\overline{v} = \sqrt{3 k_B T/m}$ is the average velocity of the particles. Considering the case of $N = 1600$ particles, at $\Gamma = 5$ we find $\omega_p \Delta t = 42.2$, which is about an order of magnitude greater than the decay time τ of $A_{\mathbf{vv}}$ [see Fig. 5(a)]. At higher values of κ we can observe a drastic increase of τ, as

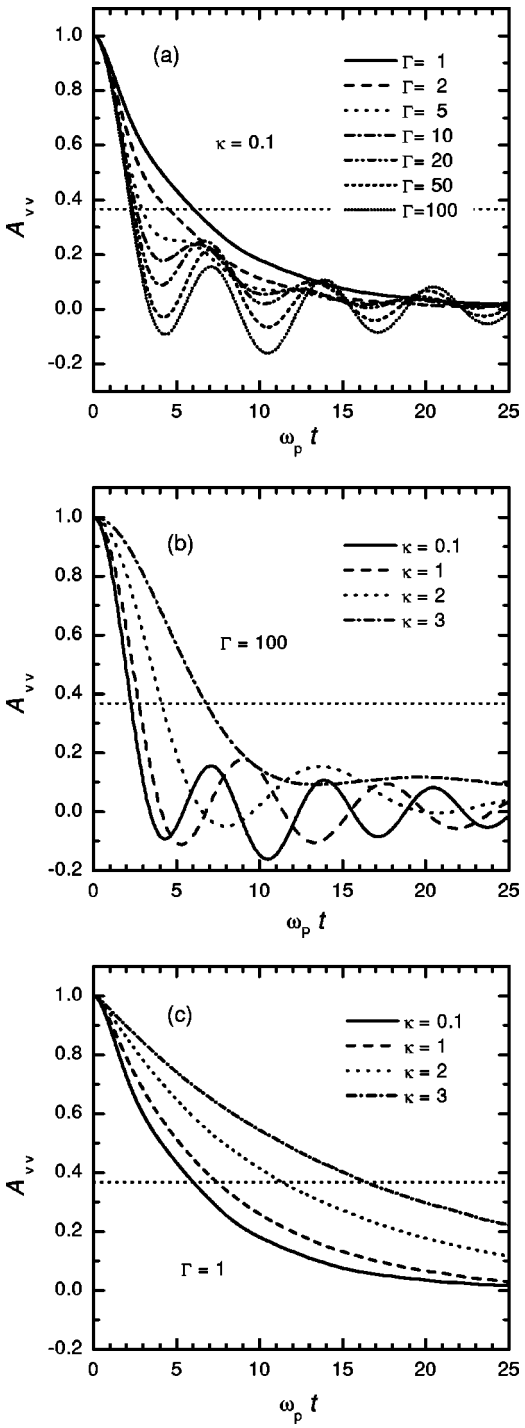

FIG. 5. Velocity autocorrelation functions (a) for different Γ values at $\kappa = 0.1$; (b) and (c) dependence on κ at $\Gamma = 100$ and $\Gamma = 1$, respectively.

shown in Figs. 5(b) and 5(c) for $\Gamma = 100$ and $\Gamma = 1$, respectively. At $\Gamma = 100$ $\omega_p \Delta t = 189$, the decay time of $A_{\mathbf{vv}}$ is well below this value, even for the greatest κ value studied. However, $\omega_p \Delta t$ becomes 18.9 for $\Gamma = 1$, and this is already in the same order of magnitude as the decay time of $A_{\mathbf{vv}}$, even for the smallest value of the screening parameter, $\kappa = 0.1$. Based on these arguments we find the low-Γ limit of the applicability of the present simulation technique to be:

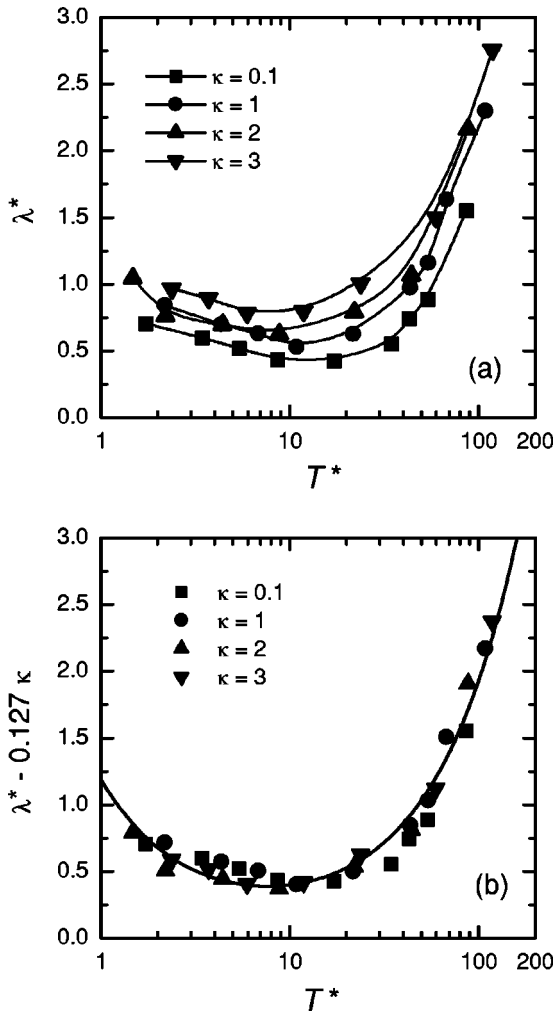

FIG. 6. (a) Reduced thermal conductivity λ^* (normalized by the Einstein frequency) as a function of the reduced temperature T^* for different κ values; (b) quasiuniversal behavior found by adding a κ-dependent term to Eq. (4), resulting in a new formula, (6), shown by the heavy line.

$\Gamma_{\mathrm{min},1600} \approx 3$ for $\kappa = 0.1$, $\Gamma_{\mathrm{min},1600} \approx 5$ for $\kappa = 1$, $\Gamma_{\mathrm{min},1600} \approx 10$ for $\kappa = 2$, and $\Gamma_{\mathrm{min},1600} \approx 20$ for $\kappa = 3$. The differences between the results obtained with different system sizes indeed show up at coupling values $\Gamma \lesssim \Gamma_{\mathrm{min}}$. For $N = 6400$ particles the lower bounds of Γ are expected to be $\Gamma_{\mathrm{min},6400} = 2^{-2/3}\Gamma_{\mathrm{min},1600}$, giving $\Gamma_{\mathrm{min},6400} \approx 2$ at $\kappa \to 0$ and $\Gamma_{\mathrm{min},6400} \approx 13$ at $\kappa = 3$.

The form (4) taken from Ref. [13] relates λ^* to the reduced temperature T^*. The plot of our λ^* data against T^*, as shown in Fig. 6(a), indicates that the above functional form cannot give an accurate fit. While it predicts the shape of the $\lambda^*(T^*)$ curve correctly and accounts for the universal behavior that the minimum of the curves at different κ values occurs nearly at the same T^* [see Fig. 6(a)], the vertical shift of the curves can only be eliminated by introducing an additional (κ-dependent) term. This way, unfortunately, the universal behavior is lost, but the resulting expression provides a more reliable approximation for the thermal conductivity

$$\lambda^* = 0.018T^* + \frac{1.05}{T^*} + 0.115 + 0.127\kappa. \tag{6}$$

The results of the present simulation (with $N = 6400$) for all κ values are shown in Fig. 6(b), together with the above expression for λ^*. One should keep in mind, however, that the validity of this expression has a limited Γ range, as discussed above.

IV. SUMMARY

We have presented nonequilibrium molecular dynamics calculations for the thermal conductivity of strongly coupled Yukawa liquids.

In the limit of low screening a very good agreement has been found between the result of the present simulations and our previous OCP data obtained from a different (transient) molecular dynamics simulation [5,6]. A reasonable agreement is also found between our data and recent results of Salin and Caillol [12] for the whole domain of the system parameters Γ and κ.

Studying the decay of the velocity autocorrelation function we have determined the Γ_{min} (applicability) limit as a function of κ and system size. Our simulations provide reliable measurements of λ in the coupling range $\Gamma \gtrsim 2$ at $\kappa = 0.1$. With increasing κ the range of applicability of the present technique was found to be $\Gamma \gtrsim 3$ at $\kappa = 1$, $\Gamma \gtrsim 7$ at $\kappa = 2$, and $\Gamma \gtrsim 13$ at $\kappa = 3$ (using $N = 6400$). The (Γ, κ) domain where the present method is applicable is limited by the ballistic trajectories of particles at low Γ and high κ values. At lower Γ values our simulation method could still work with higher number of particles, however, limitations set by computing speed did not allow us to increase the number of particles above 6400. We believe that any other (e.g., equilibrium) molecular dynamics simulations may have similar limitations set by the finite number of particles, at low Γ and high κ values, thus in any simulation studies the system size effects should be checked carefully over the whole domain of system parameters (as done in the present work).

The formula (4) proposed by Faussurier and Murillo [13], relating λ^* to the reduced temperature T^* and κ, was found to reproduce correctly the shape of the $\lambda^*(T^*)$ curves at different values of κ. We have found, however, that an additional κ-dependent term has to be added to Eq. (4) in order to give a more accurate relationship between λ^* and T^*.

ACKNOWLEDGMENTS

Support through Grant Nos. OTKA-T-34156 and MTA-NSF-OTKA-028 is gratefully acknowledged. We thank S. Hamaguchi and T. Saigo (Kyoto University) for providing their Yukawa pair correlation function data for the verification of our simulation code, and G. Bánó for his comments on the manuscript.

[1] J.-P. Hansen, I.R. McDonald, and E.L. Pollock, Phys. Rev. A **11**, 1025 (1975).
[2] P. Vieillefosse and J.P. Hansen, Phys. Rev. A **12**, 1106 (1975).
[3] J. Wallenborn and M. Baus, Phys. Lett. **61A**, 35 (1977); Phys. Rev. A **18**, 1737 (1978).
[4] B. Bernu, P. Vieillefosse, and J.P. Hansen, Phys. Lett. **63A**, 301 (1977); B. Bernu and P. Vieillefosse, Phys. Rev. A **18**, 2345 (1978).
[5] Z. Donkó, B. Nyíri, L. Szalai, and S. Holló, Phys. Rev. Lett. **81**, 1622 (1998).
[6] Z. Donkó and B. Nyíri, Phys. Plasmas **7**, 45 (2000).
[7] H. Ohta and S. Hamaguchi, Phys. Plasmas **7**, 4506 (2000).
[8] Y.H. Liu *et al.*, J. Phys. A **35**, 9535 (2002).
[9] K.Y. Sanbonmatsu and M.S. Murillo, Phys. Rev. Lett. **86**, 1215 (2001).
[10] T. Saigo and S. Hamaguchi, Phys. Plasmas **9**, 1210 (2002).
[11] G. Salin and J.-M. Caillol, Phys. Rev. Lett. **88**, 065002 (2002).
[12] G. Salin and J.-M. Caillol, Phys. Plasmas **10**, 1220 (2003).
[13] G. Faussurier and M.S. Murillo, Phys. Rev. E **67**, 046404 (2003).
[14] F. Müller-Plathe, J. Chem. Phys. **106**, 6082 (1997).
[15] D. Bedrov and G.D. Smith, J. Chem. Phys. **113**, 8080 (2000).
[16] D. Bedrov, G.D. Smith, and T.D. Sewell, Chem. Phys. Lett. **324**, 64 (2000).
[17] S. Hamaguchi, R.T. Farouki, and D.H.E. Dubin, Phys. Rev. E **56**, 4671 (1997).